

SIMULTANEOUS ABSOLUTE CALIBRATION OF THREE GEODETIC-QUALITY TIMING RECEIVERS

J. F. Plumb¹, J. White², E. Powers³, K. Larson¹, and R. Beard²

**¹ Department of Aerospace Engineering Sciences
University of Colorado, Boulder
Boulder, CO 80309, USA
Tel: 303.492.6583; Fax: 303.492.7881
E-mail: john.plumb@colorado.edu**

² U.S. Naval Research Laboratory

³ U.S. Naval Observatory

Abstract

The simultaneous calibration of three geodetic-quality timing receivers is performed with a Global Positioning System (GPS) signal simulator. Internal delays for each receiver are measured as a function of the phase difference between the one pulse per second and 20 MHz clock inputs. A calibration curve for each receiver is derived and the curves are compared.

1. INTRODUCTION

While geodetic-quality GPS carrier receivers have demonstrated high quality frequency transfer results [1], their use for precise time transfer is currently limited by our ability to calibrate the receivers. Differential calibration of geodetic-quality timing receivers has been established as the standard method for measuring relative electrical delays between two receivers [2]. To accomplish this, one receiver is designated as the reference receiver and is in constant circulation among timing laboratories. A relative calibration is performed between this receiver and the timing laboratory receiver. If time transfer between two laboratories A and B is desired, then comparisons of (A - reference) and (B - reference) are used. This method is cumbersome, and becomes more so in the event of equipment change-out. Furthermore, the stability of the calibration receiver cannot be determined.

A better solution to this calibration problem would be a repeatable method to measure the absolute electrical delays for each receiver individually. Work at the Naval Research Laboratory (NRL) has shown that by using a GPS signal simulator, the absolute delays of an Ashtech Z12-T receiver can be measured [3]. This delay depends on the difference in time of arrival at the receiver of the input 20 MHz clock signal and the one pulse per second (1 PPS) input.

2. EQUIPMENT SETUP

Three Ashtech Z12-T receivers were used in this experiment, which we designate BIPM, JPL, and CU for identification purposes. The setup for the calibration is similar to previous work done at NRL [3]. As shown in Figure 1, the GPS signal simulator produces a 1 PPS output. The pulse is sharpened by the USNO 1 PPS amplifier, allowing more accurate measurements. By inputting the simulator 1 PPS to the receivers, a fixed relationship between the simulated pseudorange code transition and the 1 PPS entering each receiver can be established. It is this fixed relationship that allows the calculation of the absolute receiver delay. A simulator auto-calibration is performed prior to data collection.

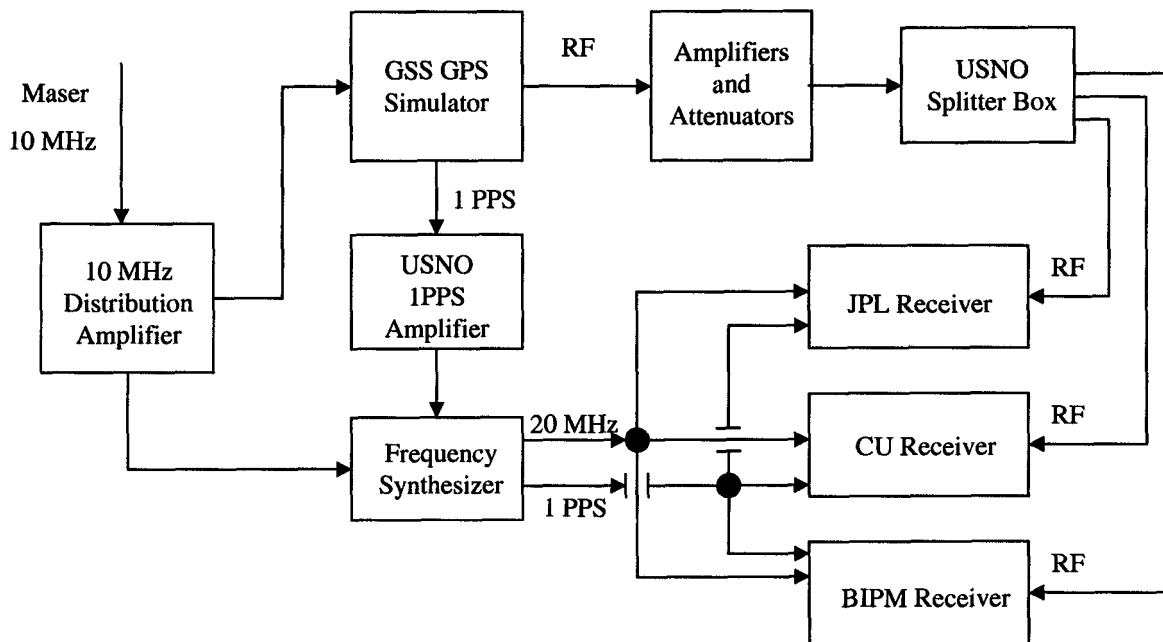


Figure 1: Equipment Setup. The simulator RF, the 20 MHz clock, and the 1 PPS signals are split and sent to all three receivers. Individual path differences are accounted for by measuring the Tick-to-Phase and Tick-to-Code Delays for the signals as they enter each receiver.

3. CALCULATING ABSOLUTE RECEIVER DELAY

3.1 OBSERVABLES

For the purposes of this paper, C1 denotes the pseudorange observables from the C/A code transmitted on carrier frequency f_1 . P1 denotes the P-code pseudorange observable on frequency f_1 . P2 denotes the pseudorange observable on frequency f_2 . P3 denotes the ionosphere-free linear combination of P1 and P2.

The frequencies f_1 and f_2 are 1575.42 MHz and 1227.60 MHz, respectively.

3.2 MEASURING THE TICK-TO-CODE DELAY

Simulating a satellite range of zero, a fast digital oscilloscope is used to measure the delay between the arriving simulated pseudorange code segment transition and the rising tick of the GPS signal simulator's generated 1 PPS. This delay is referred to as the Tick-to-Code (TtC) delay (Figure 2). This delay, inherent to the simulator and the electrical path of Figure 1, represents the difference between the satellite clock and the receiver clock. It will be subtracted from the ranges reported by the receiver. Given real data, the input 1 PPS would be from the timing laboratory's clock, and the TtC value would vary with time. Because the simulator generates the 1 PPS in our experiment, the pulses are fixed with respect to the simulated pseudorange. Therefore, for each receiver, the TtC delay is constant. In all cases, the Tick-to-Code delays were measured at the inputs to the back of the receiver (Table 1).

| | <i>BIPM</i> | <i>JPL</i> | <i>CU</i> |
|----|----------------|----------------|-----------|
| C1 | 22.64 ns | 15.34 ns | 16.07 ns |
| P2 | 26.34 ns | 19.04 ns | 19.07 ns |
| P1 | (not measured) | (not measured) | 15.88 ns |

Table 1. Difference between time of arrival of pseudorange code segment transitions and the time of the rising 1 PPS signal measuring 1 volt for each of the three receivers. This value is referred to as the "Tick-to-Code" delay, or TtC. Positive numbers mean the code transition occurred after the rising 1 PPS signal. Values are repeatable within ± 0.02 ns.

3.3 MEASURING THE TICK-TO-PHASE DELAY

The important aspect of the Ashtech Z12-T that allows absolute calibrations to be performed is the repeatability of the internal reference. The Z12-T requires two external inputs: a 1 PPS signal and a 20 MHz clock signal. The 20 MHz zero crossing that immediately follows the rising tick of the 1 PPS signal marks the internal reference (zero) time for the receiver. Whether this internal reference is marked by the rising or falling 20 MHz zero can be determined by opening the receiver case and inspecting the jumper on the circuit board: its position is clearly marked as rising or falling. All three of the receivers used in this experiment were configured for the rising zero. By carefully selecting the time difference between the input 20 MHz clock rising zero and the input 1 PPS signal, the internal timing reference becomes repeatable. This time difference is called the Tick-to-Phase delay, denoted as TtP in this paper (Figure 3).

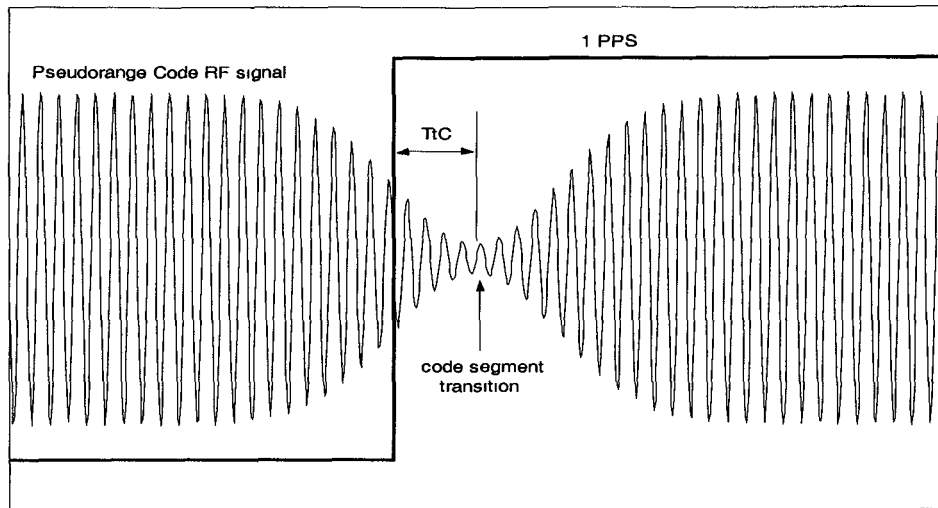


Figure 2. Measuring the Tick-to-Code Delay. The time from the 1 PPS signal until the code segment transition is the Tick-to-Code Delay (TtC). This measurement is made when simulating a zero range to the satellite. The figure shows a positive TtC.

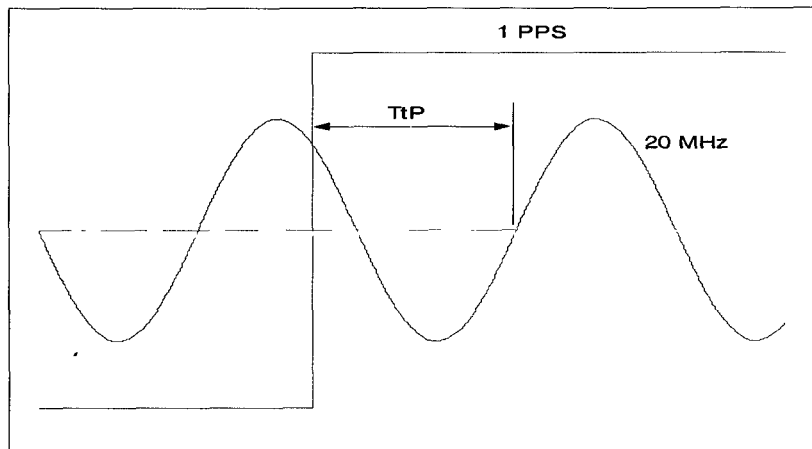


Figure 3. Measuring the Tick-to-Phase Delay. The time from the rising 1 PPS tick until the next rising zero of the 20 MHz clock signal is the Tick-to-Phase Delay (TtP). This measurement is taken as the signals enter the receiver.

3.4 CALCULATION OF ABSOLUTE RECEIVER DELAY

Because the Tick-to-Code delay is known, by varying the Tick-to-Phase delay a repeatable calibration curve for each receiver can be generated. The range reported (RR) by the receiver is taken directly from the RINEX files. This range will be too large by the combination of the receiver delay and the Tick-to-Code delay. Using the true simulated range (TR) to the receiver (recorded by the simulator) and the

measured difference between the 1 PPS signal and the pseudorange code transition (TtC), the receiver delay is calculated as follows:

$$RR - TR - TtC = \text{Receiver Delay (TtP)}$$

The receiver delay is a function of the input Tick-to-Phase value.

4. EXPERIMENT

The frequency synthesizer in Figure 1 converts the input 10 MHz clock into a 20 MHz clock output. By triggering this output with the 1 PPS signal, we use the synthesizer to shift the relative phase of the 20 MHz clock and 1 PPS input signals. Tick-to-Phase was shifted in increments of 72 degrees, which corresponds to increments of 10 ns for a 20 MHz signal. The receivers collected data at each phase increment for approximately 20 minutes. Simulator ionospheric and tropospheric delays were turned off; this was essential for calculating the delay due only to the receiver.

5. RESULTS

5.1 C1 AND P2 ABSOLUTE DELAYS

C1 and P2 code delays for each receiver are given as a function of the input Tick-to-Phase delay in Figure 4. To achieve these results, the receiver delay was calculated for each satellite at each observation epoch by subtracting the simulator generated “truth range” and the measured Tick-to-Code delay from the receiver’s reported range to each satellite. Each 20-minute run was then analyzed for an average delay, with outliers greater than three times the standard deviation removed. This process was iterated until no outliers remained. On all three receivers, the internal delays due to one satellite (PRN 25) were significantly different from all other satellites; this was considered to be a problem with the simulator. All data from PRN 25 were discarded for this experiment. However, this had little effect on the results since most delays calculated for PRN 25 were outlier values.

We note that the difference in delays between receivers varies significantly. In order to achieve sub-nanosecond calibrations, each receiver must be calibrated individually.

Table 2 shows the calculated slopes for each calibration curve. Slopes were calculated by using a least squares fit to the average delay at each Tick-to-Phase interval. Note that in each case the expected slope is (-1): for each 1 nanosecond increase in Tick-to-Phase, the receiver delay should decrease by 1 nanosecond.

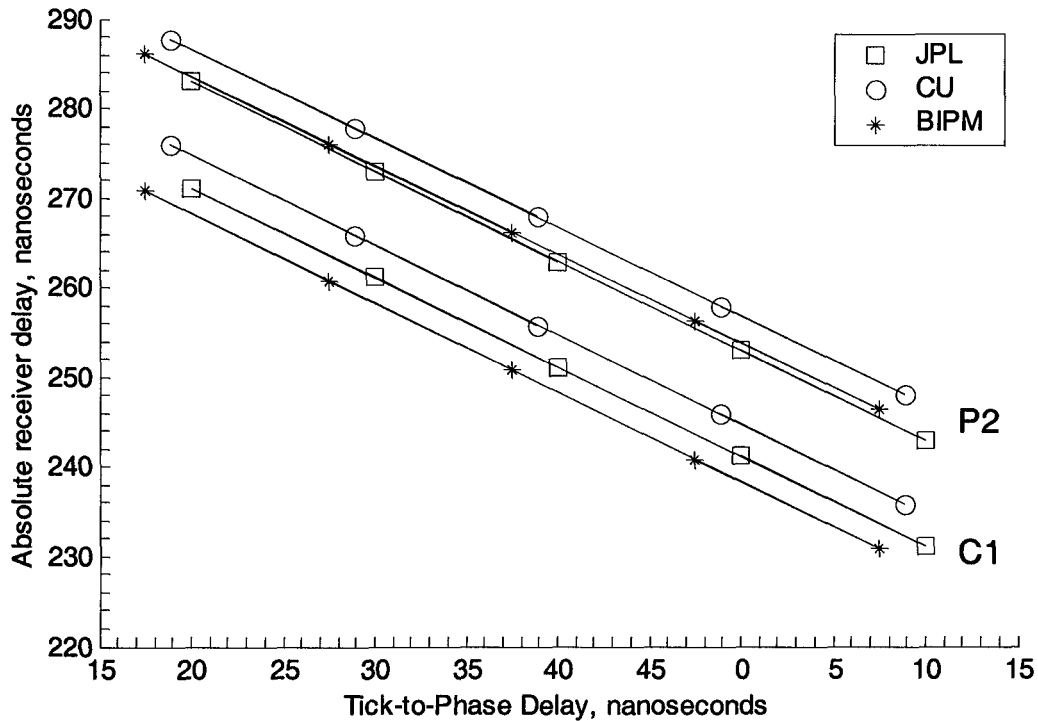


Figure 4. C1 and P2 pseudorange code receiver delays as a function of the input Tick-to-Phase delay. In all cases, the delay for frequency L2 is longer than frequency L1. The Tick-to-Phase delay of zero nanoseconds occurs where we expect a delay of 50 ns to be. Because the input clock is at 20 MHz (1 cycle = 50 ns), a 50 ns Tick-to-Phase delay is the same as a Tick-to-Phase delay of zero.

| Calibration curve | <i>BIPM</i> | <i>JPL</i> | <i>CU</i> |
|-------------------|-------------|------------|-----------|
| C1 | -0.9991 | -0.9979 | -1.0029 |
| P2 | -0.9931 | -1.0000 | -0.9940 |
| P3 | -1.0085 | -0.9946 | -1.0165 |

Table 2. Slopes of calibration curves. The standard deviation for each estimate is ± 0.17 . Units are ns/ns.

Examining Figure 4, we note that the Tick-to-Phase value of zero is located on the x-axis where we expect 50 ns to be. Furthermore, the curves continue out to at least 7 ns (which is where we expect 57 ns to be located.) The 20 MHz clock signal repeats every 50 ns. We determine the Tick-to-Phase delay by measuring the relationship of the two signals as they enter the receiver; the internal electrical path of the receiver is not taken into account. From entering the receiver until the signals reach the component marking the internal reference, the electrical path of the 1 PPS signal is at least 7 ns longer than the 20 MHz signal's path. Any rising zero entering the receiver within 7 ns of the rising 1 PPS will be trailing that pulse when the signals arrive at the marking component. The next rising zero, which occurs 50 ns (one full cycle) later, will be the first rising zero arriving after the tick. For instance, if the measured Tick-to-Phase delay is 5 ns, the rising zero at 55 ns will mark the internal timing reference.

The exact amount each receiver delays its 1 PPS signal relative to its 20 MHz clock is unknown, but the value is bounded by the 10 ns gap produced by the data collection method. Thus, the JPL receiver delays its 1 PPS signal between 10 and 20 ns longer than its 20 MHz clock signal. The Tick-to-Phase value that causes this crossover could be determined by finer resolution data collection increments between 10 and 20 ns.

5.2 IONOSPHERE-FREE DELAY

The Tick-to-Code delay for the P1 code was only measured for the CU receiver. The P1 delay, when calculated, matched the C1 delay within the calculated variance. It is reasonable to assume that this will hold true for all three receivers. Because the ionospheric delay is frequency-dependent, P3, the ionosphere-free linear combination of P1 and P2, can be calculated. Knowing the absolute delays for the P1 and P2 pseudorange codes, the effective ionosphere-free P3 delay is calculated in the same manner:

$$P3 \text{ delay} = \frac{f_1^2}{f_1^2 - f_2^2} * P1 \text{ delay} - \frac{f_2^2}{f_1^2 - f_2^2} * P2 \text{ delay}$$

Figure 5 shows the ionosphere-free results for the CU receiver. Utilizing the assumption that the C1 and P1 receiver delays are equal, Figure 6 shows ionosphere-free delays for all three receivers.

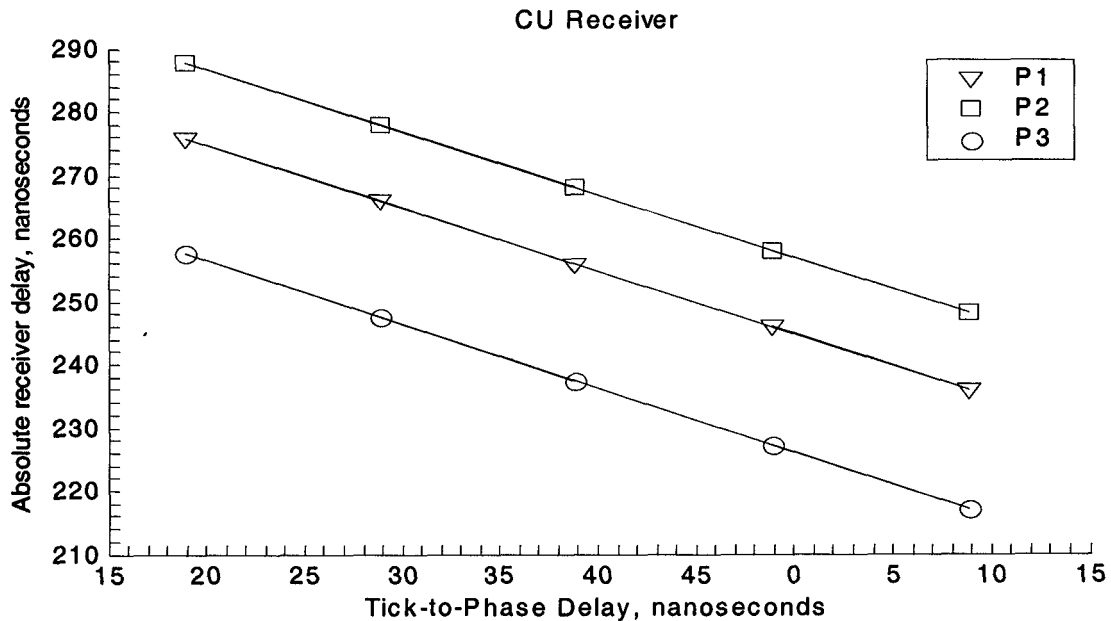


Figure 5. The CU receiver effective ionosphere-free delay for the P3 observable is graphed along with the P1 and P2 delays.

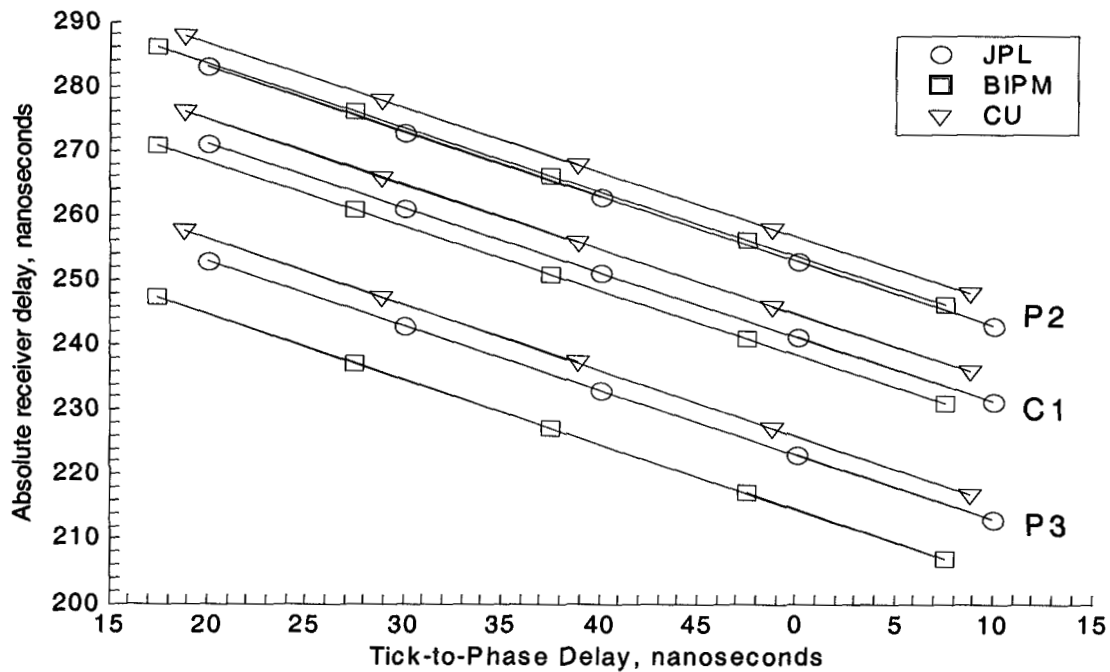


Figure 6. Plotting the ionosphere-free delay for all three receivers. For the JPL and BIPM receivers, this delay was calculated using C1 and P2 delays vice P1 and P2 delays. Therefore, P3 delays for these two receivers are only accurate if the P1 and C1 delays are identical.

5.3 DELAYS IN EQUATION FORM

For ease of calculation, the results for C1 and P2 are presented here in equation form. In order to determine the absolute delay of the receiver, simply enter the Tick-to-Phase delay in nanoseconds and compute. The bounds due to the data collection method are given. As discussed in Section 5.1, a measured delay of 5 ns must be represented as 55 ns when the data are presented in this form. These results were found by a least-squares best fit to the data using the expected slope of (-1). Results are accurate to the sub-nanosecond level. As in Figure 6, P3 delays for the JPL and BIPM receivers are only accurate if C1 and P1 delays prove to be identical.

CU Receiver: (Applicable interval: 18.9 ns to 58.9 ns)

$$\text{C1 delay} = 294.75 - \text{TtP}$$

$$\text{P2 delay} = 306.80 - \text{TtP}$$

$$\text{P3 delay} = 276.13 - \text{TtP}$$

JPL Receiver: (Applicable interval: 20.0 ns to 60.0 ns)

$$\text{C1 delay} = 291.20 - \text{TtP}$$

$$\text{P2 delay} = 303.01 - \text{TtP}$$

$$\text{P3 delay} = 272.95 - \text{TtP}$$

BIPM Receiver: (Applicable interval: 17.5 ns to 57.5 ns)

$$\text{C1 delay} = 288.36 - \text{TtP}$$

P2 delay = 303.69 - TtP

P3 delay = 264.66 - TtP

6. SUMMARY

A calibration curve can be generated for geodetic-quality timing receivers. These receivers can be operated over a wide range of Tick-to-Phase delay values; knowing this value allows the receiver absolute delay to be calculated in a straightforward manner. Once absolute delays for P1 and P2 pseudorange codes are known, the ionosphere-free delay can also be calculated. Individual receivers vary enough to require individual calibrations for their delays.

7. REFERENCES

- [1] K. Larson, J. Levine, L. Nelson, and T. Parker, 2000, "Assessment of GPS Carrier-Phase Stability for Time-Transfer Applications," **IEEE Transactions on Ultrasonics, Ferroelectrics, and Frequency Control**, UFFC-47, 484-494.
- [2] G. Petit, Z. Jiang, P. Uhrich, and F. Taris, 2000, "Differential Calibration of Ashtech Z12-T Receivers for Accurate Time Comparisons," in Proceedings of the 14th European Frequency and Time Forum (EFTF), 14-16 March 2000, Torino, Italy, pp. 40-44.
- [3] J. White, R. Beard, G. Landis, G. Petit, and E. Powers, 2001, "Dual Frequency Absolute Calibration of a Geodetic GPS Receiver for Time Transfer," in Proceedings of the 15th European Frequency and Time Forum (EFTF), 6-8 March 2001, Neuchâtel, Switzerland (FSRM, Neuchâtel), pp. 167-172.